ELSEVIER

Journal of Chromatography A, 772 (1997) 3–17

JOURNAL OF CHROMATOGRAPHY A

Bidirectional isotachophoresis in open-tubular, untreated fused-silica capillaries

Jitka Caslavska, Wolfgang Thormann*

Department of Clinical Pharmacology, University of Bern, Murtenstrasse 35, CH-3010 Bern, Switzerland

Abstract

A dynamic computer model for simulation of open-tubular capillary electrophoresis, which includes in situ calculation of electroosmosis along the fused-silica capillary and allows the application of imposed flow, has been applied to the characterization of bidirectional isotachophoretic systems in the presence of a cathodic plug flow. Electroosmosis is calculated based upon the voltage gradient and a wall titration curve (mobility vs. pH), which takes into account the dissociation of surface groups of the inner capillary wall, a wall mobility at full dissociation (high pH) and the non-vanishing surface charge at low pH. For model bidirectional isotachophoretic configurations between pH 4 and 9, simulation data reveal the complete loss of the cationic zones at the cathodic column end and the asymptotic formation of a stationary steady-state anionic zone configuration in which electrophoretic and electroosmotic zone displacements are opposite and of equal magnitude. The position of the stationary boundary between the leading compound and sample is predicted to be dependent on the pH of the system, applied imposed co-flow, and sample composition. Cationic sample trains can readily be detected with a sensor placed towards the cathodic end of the capillary. However, without imposed co-flow, anionic structures are shown to be detectable only at elevated pH values. For detection at 73 or 90% of column length, net cathodic displacement rates per cm column length of about $\geq$10 and $\geq$15 μm/s, respectively, are required. Electroosmosis-based displacement of these magnitudes are predicted only for pH$\geq$6 and alkaline systems, respectively. For a detector placed at 73% of column length, qualitative agreement between experimental data and simulation results is obtained. Practical aspects of the bidirectional isotachophoretic systems are discussed with data of urinary salicylate and two of its metabolites.

Keywords: Isotachophoresis; Computer simulation; Electroosmosis; Bidirectional electrophoresis

1. Introduction

Electrophoretic transport is bidirectional [1], an aspect that has been scarcely explored in modern-type capillary isotachophoresis (cITP). The simultaneous formation of cationic and anionic boundaries and sample trains in the presence of suitable discontinuous electrolyte systems, however, was discussed many years ago using the Tiselius apparatus (for a review see Ref. [2]) or set-ups comprising paper strips [3]. More recently, dual isotachophoretic systems have been characterized in capillary-type instrumentation with multiple and scanning detectors [4,5] and in continuous flow electrophoretic devices [5]. Furthermore, fifteen bidirectional isotachophoretic electrolyte systems covering the pH range 3.5–10 have been proposed [6].

In the past few years, instrumentation for electrokinetic separations in open-tubular fused-silica capillaries of very small I.D. (25–75 μm) became available and papers reporting their use for cITP appeared in the literature [7–16]. The longitudinal electroosmotic flow established in these capillaries was found not to disturb isotachophoretic zone formation,

*Corresponding author.

PII S0021-9673(97)00140-4

but to make quantitation more difficult than in classical cITP performed in narrow bore plastic tubes. In the presence of electroosmosis, it is particularly difficult, if not impossible, to maintain constant solute transport along the capillary column [9,13,16]. Electroosmosis is mainly dependent upon surface charge of the capillary wall (pH), the electric field determined by current density and conductivity (composition of the solutions present in the capillary) and viscosity. These three parameters are typically constant in capillary zone electrophoresis in which the sample is the only discontinuous element present, but may vary in configurations comprising discontinuous buffer systems, such as capillary isoelectric focusing and cITP. Recently, a dynamic model for computer simulation of electroosmosis in capillary electrophoresis, based upon the dissociation of the silanol surface groups of the capillary wall, was developed [17] and successfully applied to the description of capillary zone electrophoresis [17] and cITP [16]. Furthermore, this model was extended to account for residual electroosmosis at low pH values, which permitted the simulation of capillary isoelectric focusing in the presence of electroosmosis [18]. The option of applying imposed plug flow along the capillary, as described previously [19], has also been included.

Using the extended computer model with the option of imposing additional plug flow, the temporal behavior of solute transport in bidirectional cITP has been investigated and compared to experimental data obtained in open-tubular, untreated fused-silica capillaries of 75 μm I.D. Bidirectional electrolyte systems at various pH values were chosen from those described by Hirokawa [6]. Furthermore, application of these configurations to the analysis of urinary salicylate and its metabolites in instruments with a single detector placed towards the cathodic end of the column are described.

2. Experimental

2.1. Chemicals

The chemicals used were of analytical or research grade. Sodium salicylate, procaine chloride and tris(hydroxymethyl)aminomethane (Tris) were purchased from Merck (Darmstadt, Germany). 2-Amino-2-methyl-1,3-propanediol (ammediol), 2-(N-morpholino)ethanesulphonic acid (MES), glycylglycine, β-alanine, histidine and *o*-hydroxyhippuric acid (salicyluric acid, SUA) were obtained from Sigma (St. Louis, MO, USA). Sodium acetate and 2,5-dihydroxybenzoic acid (gentisic acid, GA) were from Fluka (Buchs, Switzerland).

2.2. Computer simulations

The program was executed on an Excel AT 486 computer (Walz Computer, Bern, Switzerland) or a notebook 486 computer (Data 2000, Bern, Switzerland) running at 50 and 33 MHz, respectively. The components' input data for simulation are summarized in Table 1. All simulations were performed with a 3-cm separation space divided into 600 segments of equal length and with an applied constant voltage of 30 V. The compositions of the anolytes and catholytes used are summarized in Table 2. The sample was composed of 35 m*M* sodium salicylate and 100 m*M* procaine chloride and was applied at the anodic end of the column. Initially, the capillary was filled with catholyte (98% of column length), sample (1%) and anolyte (1%). The wall titration data presented in Fig. 1 were employed as the input for simulation of electroosmosis. The function describing the pH dependence was constructed as described previously [18] and is based upon a wall pK_a of 5.5, a wall mobility (at full

Table 1
Physico-chemical input parameters used for simulation

Compound	pK_{a_1}	pK_{a_2}	Mobility ($\times 10^{-8}$ m^2/V s)	Ref.
β-Alanine	3.60	10.19	3.63	[1]
Histidine	6.04	9.17	2.85	[1]
Tris	8.08		2.95	[20]
Procaine	9.00		2.57	[21]
Ammediol	8.78		3.20	[20]
Acetic acid	4.76		4.12	[1]
Salicylic acid	2.94		3.53	[20]
MES	6.13		2.68	[20]
Glycylglycine	3.15	8.4	3.15	[20]
Na^+			5.19	[1]
Cl^-			7.91	[1]
H^+			36.27	[1]
OH^-			19.87	[1]

Table 2
Electrolyte systems studied for dual isotachophoresis in fused-silica capillaries

System	Anolyte (10 m*M* HCl+20 m*M* cationic buffer)			Catholyte (10 m*M* NaOH+20 m*M* anionic buffer)		
	Cationic buffer	pH	Conductivity (S/m)	Anionic buffer	pH	Conductivity (S/m)
1	β-Alanine	3.62	0.1189	Acetic acid	4.76	0.0905
2	Histidine	6.04	0.1039	MES	6.13	0.0760
3	Tris	8.08	0.1048	Glycylglycine	8.40	0.0805
4	Ammediol	8.78	0.1073	Histidine	9.17	0.0779

dissociation) of $6.5 \cdot 10^{-8}$ m^2/V s and a residual mobility at low pH of $1.0 \cdot 10^{-8}$ m^2/V s. Imposed plug flows towards the cathode were between 0 and 50 μm/s. For making plots, the data were imported into SigmaPlot Scientific Graphing Software, version 4.01 (Jandel Scientific, Corte Madera, CA, USA).

2.3. Instrumentation and experimental conditions

Electrokinetic measurements were made with the Prince apparatus (Lauerlabs, Emmen, Netherlands), an instrument that features the possibility of applying hydrodynamic co- or counterflow during an experiment. For on-column solute detection, the Prince was interfaced with a fast forward-scanning UVIS 206 PHD detector (Linear Instruments, Reno, NV, USA), which was modified for simultaneous fluorescence and absorbance detection [22]. In the combined detection mode, UV detection and fluorescence excitation were effected at 220 nm, whereas fluorescence emission was measured using a 450-nm band pass filter. In the fast scanning UV absorption mode, multiwavelength patterns were monitored between 195 and 320 nm at 5 nm intervals. Fused-silica capillaries (Polymicro Technologies, Phoenix, AZ, USA) of 75 μm I.D. and 48 cm (66 cm) effective (total) length were employed. The temperature of the capillary was kept at 35°C. The applied voltage was 20 kV (anode on the sampling side). Prior to use, capillaries were etched with 1 *M* NaOH and rinsed with 0.1 *M* NaOH for about 20 min each. If not otherwise stated, capillary conditioning was effected by rinsing with catholyte for 3 min using a positive pressure of 2000 mbar and sample injection was carried out by applying a positive pressure of 20 mbar for 0.1 min, which provided an initial sample plug of about 3.2 mm (about 0.5% of the capillary length). The imposed co-flow generated via application of positive pressure between 10 and 50 mbar was found to be linearly dependent on pressure and determined to provide a cathodic flow of about 0.23 cm/min and mbar.

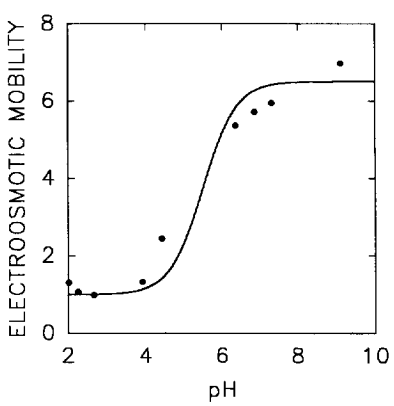

Fig. 1. Wall titration data (solid line) employed for calculation of electroosmosis. The dots represent experimental values taken from Ref. [17]. Mobility units: 10^{-8} m^2/V s.

3. Results and discussion

3.1. Characterization of a bidirectional isotachophoretic configuration at alkaline pH by computer simulation

First, bidirectional cITP at alkaline pH, i.e. in a region with full dissociation of the capillary wall, was investigated. The configuration described in detail comprised 10 m*M* HCl–20 m*M* Tris (pH 8.08) as the anolyte and 10 m*M* NaOH–20 m*M* glycylglycine (pH 8.40) as the catholyte (system 3 of Table 2). In this system, chloride and sodium act as

anionic and cationic leading compounds, respectively (anionic and cationic leaders in Fig. 2A are denoted by L_A and L_C, respectively). Glycylglycine and Tris are the corresponding displacing constituents of the terminators, denoted by T_A and T_C, respectively. The sample was composed of sodium salicylate (35 m*M*) and procaine chloride (100 m*M*) and was placed between the two buffers with the initial sample position at the anodic end of the capillary (i.e. between 1 and 2% of column length; Fig. 2A, bottom graph). Upon application of power, salicylate (S) and procaine (P) migrate electrophoretically towards the anode and cathode, respectively, thereby forming isotachophoretic zones with self-sharpening boundaries. Furthermore, the whole liquid is being transported towards the cathode by electroosmosis. Employing a wall p*K* and mobility of 5.5 and $6.5 \cdot 10^{-8}$ m^2/V s, respectively, the model predicts (at least initially) that the net transport of both sample compounds is towards the cathode (Fig. 2A). The predicted electroosmotic flow of 65 μm/s appears to be stronger than the anionic, isotachophoretic migration rate of chloride and salicylate. After 4 min of current flow (top graph of Fig. 2A), all boundaries are predicted to be fully established. Data representing the pH and conductivity distributions at 4 min of current flow are depicted in panel B of Fig. 2. Furthermore, corresponding profiles for the ionic strength and electroosmosis are presented in panel C. The electroosmotic flow data predicted for each capillary segment do not reflect a real, physical distribution, but provide insight into the pumping activity of each zone. Compared to the leaders, terminating zones are shown to contribute more strongly to the net electroosmotic flow. Conductivity and ionic strength are significantly lower in the terminators, whereas the pH is predicted not to vary much along the column.

The data presented in Fig. 2D represent computer-predicted concentration profiles of salicylate and procaine between 4 and 24 min of current flow (at 2.5 min intervals). They show that procaine is leaving the capillary at the cathodic end (before 6.5 min of current flow) and that the net displacement of salicylate decreases with time. As a matter of fact, salicylate is predicted to become immobile after about 24 min of current flow. Moreover, the current density (solid line in Fig. 2E) is shown to become invariant as the electrophoresis time approaches 24 min. As described in detail previously [16], a stationary steady state zone configuration, characterized by an equilibrium between anodic isotachophoretic zone transport and cathodic electroosmosis, is produced. The net electroosmotic flow is predicted to be a constant 65 μm/s (broken line in Fig. 2E), corresponding to 6.5 μm/s per unit of applied electric field, which equals the wall mobility of $6.5 \cdot 10^{-8}$ m^2/V s. Under the employed conditions, the chloride–salicylate boundary is predicted to become immobile at about 90% of column length.

3.2. Experimental validation at alkaline pH

Multiwavelength experimental data obtained without and with a sample composed of 35 m*M* sodium salicylate and 100 m*M* procaine chloride are presented in panels A and B of Fig. 3, respectively. The data reveal that both the cationic and the anionic cITP zone structures reached the detector placed at about 73% of column length without application of co-flow. At low detection wavelengths, all four buffer zones could be monitored and properly assigned to those predicted by computer (compare Fig. 2A and Fig. 3A). Furthermore, salicylate and procaine could be detected within the entire range of wavelengths of 195 to 320 nm (Fig. 3B). The data presented in panels C and D of Fig. 3 represent computer-predicted (lower graphs) and experimental (upper graphs) data for solute detection at 220 and 300 nm, respectively, and with the detector positioned at 73% of column length. Considering that glycylglycine, Tris, salicylate and procaine are contributing to the detector response at 220 nm and that the detection cell is initially filled with catholyte containing glycylglycine (Table 2), response factors in relation to glycylglycine were determined spectrophotometrically. Salicylate, procaine and Tris were found to absorb 6.11-, 7.78- and 0.44-fold more strongly, respectively, than glycylglycine at that wavelength. Thus, the compounds' concentrations were multiplied by these factors and added up to provide the emulated detector signal. For presentation purposes, the obtained number (in m*M*) was divided by 300 (panel C of Fig. 3). Accordingly, for detection at 300 nm, only the responses of salicylate (factor 33) and procaine (factor 150) were consid-

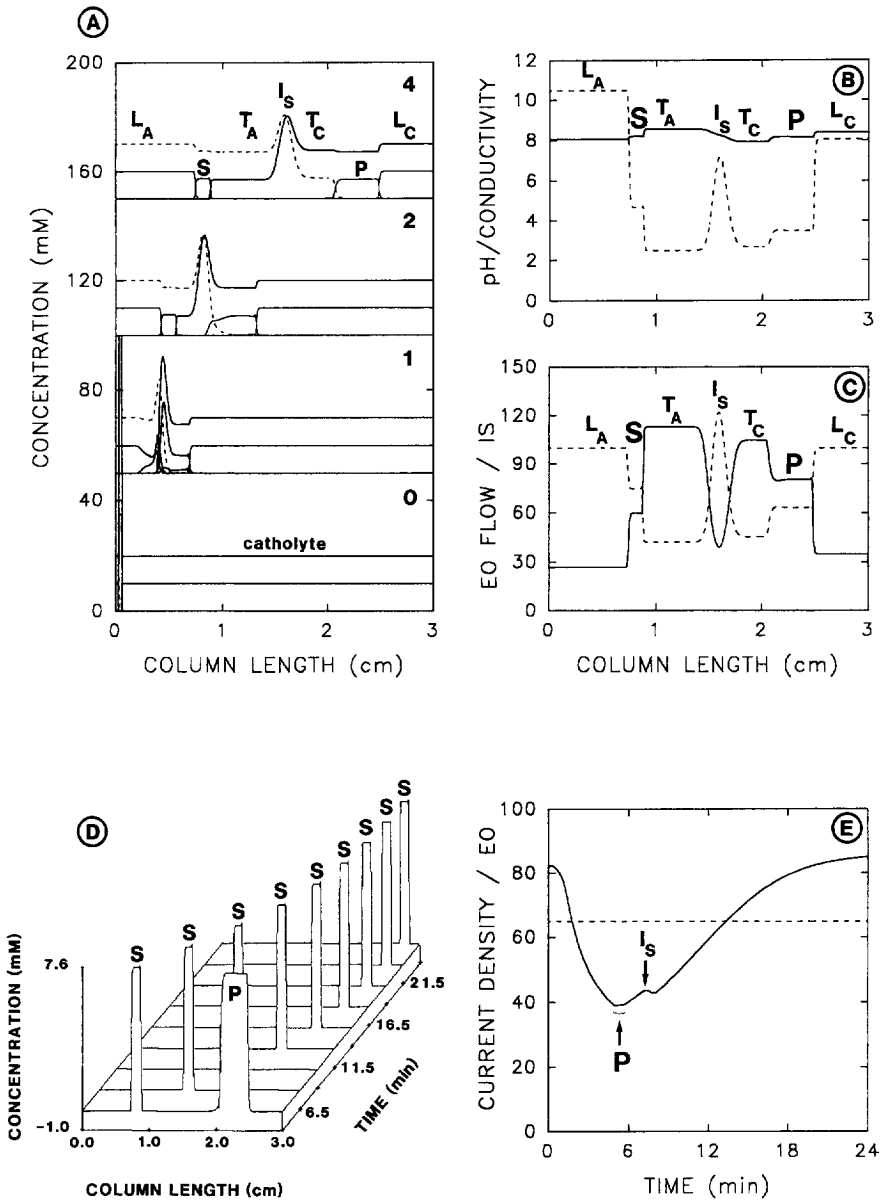

Fig. 2. Simulation data for bidirectional isotachophoresis at pH 8 (system 3 of Table 2). (A) Concentration profiles for 0, 1, 2 and 4 min of current flow (from bottom to top, depicted with a *y*-axis offset of 50 m*M*). The counter component of the anionic leader (Tris) is depicted as a broken line. (B) pH (solid line) and conductivity (broken line; units: S/m, values multiplied by 100) distributions after 4 min of current flow. (C) Electroosmosis (solid line; μm/s) and ionic strength, IS (broken line; units: m*M*, values multiplied by ten) after 4 min of current flow. (D) Concentration profiles of salicylate (S) and procaine (P) between 4 and 24 min of current flow (interval 2.5 min). (E) Temporal behavior of current density (solid line; units: A/m^2) and net electroosmotic flow (broken line; units: μm/s). L_A and T_A refer to the anionic leader and terminator, respectively. Corresponding cationic zones are denoted by L_C and T_C, respectively. I_S refers to the fluid element originally occupied by the sample (diffusive boundary system).

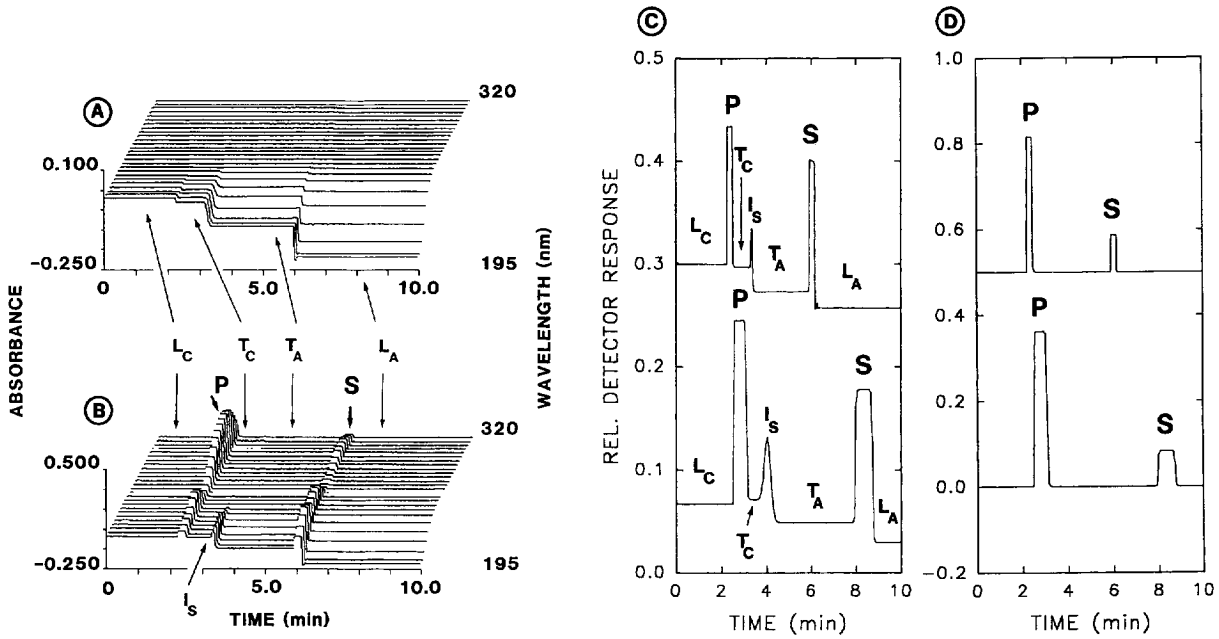

Fig. 3. Bidirectional multiwavelength cITP data of (A) blank and (B) procaine and salicylate at pH 8. Panels C and D depict computer-simulated (lower graphs with a converted time scale) and experimental pherograms (top graphs) for detection at 220 and 300 nm, respectively. Experimental data in panels C and D are drawn with a *y*-axis offset of 0.3 and 0.5 AU, respectively. For an explanation of the simulation data refer to text. Symbols are as in Fig. 2.

ered, added up and, for the sake of presentation, the obtained signal (m*M*) was divided by 3000. Furthermore, for close comparison of simulation and experimental data, the following has to be considered. In the experiment, a voltage gradient of 300 V/cm was applied, this being 30 times larger than that employed for simulation. On the other hand, the column length used for computer prediction was 22-fold shorter than that used experimentally. Thus, time scales of prediction and experimental validation should be comparable when the simulation time scale is divided by 1.364, the ratio of the two scaling numbers. As is shown for the data presented in Fig. 3C–D, this was found to be essentially true. One small difference should be noted. In the experiment, the initial sample plug length was about 0.5% of the column length, whereas a 1% sample zone was employed for simulation. Thus, predicted zones are somewhat broader than those that were observed experimentally. With 600 segments along the column, a 0.5% sample zone cannot be treated properly. On the other hand, a finer segmentation would have inconveniently increased the computer time required.

The computer-predicted, temporal behavior of the current density is depicted in Fig. 2E. Under constant voltage conditions (as applied here), the current initially decreases sharply. As the cationic isotachophoretic procaine zone is leaving the column (between about 5.0 and 5.8 min, marked by a P in Fig. 2E), the current is predicted to decrease only slightly. Thereafter, an increase in the current is predicted until the fluid element of the initial sample (denoted by I_S in Fig. 2E) reaches the capillary end at about 7.5 min. Then, after a slight decrease, the current density increases to a level that is slightly above the initial value. This overall behavior was observed as well. For the data depicted in Fig. 3B, the current was determined to drop from an initial value of 11.9 to 4.8 μA at the time of detection of the initial transition (diffusive zone marked by I_S in Fig. 3B–C). Thereafter, the current increased to a value of 13.6 μA at 10 min of current flow, thus demonstrating good agreement. Overall, for electrolyte system 3 listed in Table 2, qualitative agreement between simulation and experimental data was obtained. The same was found to be true for a

configuration around pH 9 (system 4 of Table 2). With this configuration, however, procaine did not form an isotachophoretic zone and migrated zone electrophoretically within the cationic terminating electrolyte, T_C (data not shown). Furthermore, the anionic chloride–salicylate boundary became immobile at about 93% of column length, this being at a somewhat more cathodic position compared to that encountered at pH 8 (90%). The net electroosmotic flow for the two systems, however, was predicted to be equal.

3.3. Bidirectional isotachophoresis at pH 6

The second detailed investigation was performed at pH 6, a buffer pH around the pK_a of the silanol groups of the capillary wall (Fig. 1). Histidine and MES were used as counter compounds in the anolyte and catholyte, respectively (system 2 of Table 2). Compared to the alkaline buffers described above, the two isotachophoretic test compounds were predicted and observed to have similar behavior (Figs. 4 and 5). Furthermore, the anionic part of this electrolyte system is comparable to that employed previously for describing the attainment of a stationary isotachophoretic steady state within a fused-silica capillary [16], for monitoring of salicylate in urine and serum [14] and for characterizing the anionic isotachophoretic behavior of dyes [7,12]. The simulation data presented in Fig. 4 represent concentration profiles (panel A), pH and conductivity distributions (panel B) and calculated electroosmosis and ionic strength values for each segment (panel C). With the exception of the lower pH value, the distributions of the various properties are very similar to those predicted for an electrolyte system at alkaline pH (Fig. 2). With a sample composed of 35 m*M* sodium salicylate and 100 m*M* procaine chloride, qualitative agreement between experimental and simulation data was obtained (Fig. 5C). For data comparison, the simulation time scale was again divided by 1.364 (see above) and the detector response for 220 nm was constructed by using the response factors of 1.00, 1.38 and 1.75 for histidine, salicylate and procaine, respectively, and by dividing the sum of the concentrations (m*M*) by 100. For the pH 6 system, the chloride–salicylate boundary was predicted to become immobile at about 83% of the

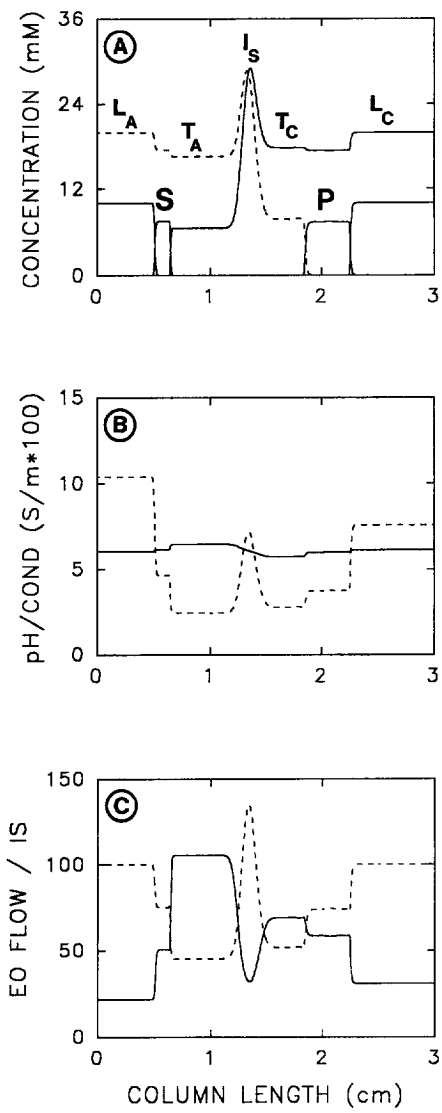

Fig. 4. Simulation data at pH 6 (system 2 of Table 2) and after 4 min of current application with (A) concentration profiles, (B) pH (solid line) and conductivity (broken line; units: S/m, values multiplied by 100) distributions, and (C) electroosmotic flow (solid line; units: μm/s) and ionic strength (broken line; units: m*M*, values multiplied by ten) data for each column segment.

column length (data not shown). As is shown with the data presented in Fig. 5C, a detector placed at 73% of the column length was able to monitor the salicylate zone. In view of the approximated wall titration curve used for simulation of electroosmosis, this is a remarkable agreement. Electroosmosis is

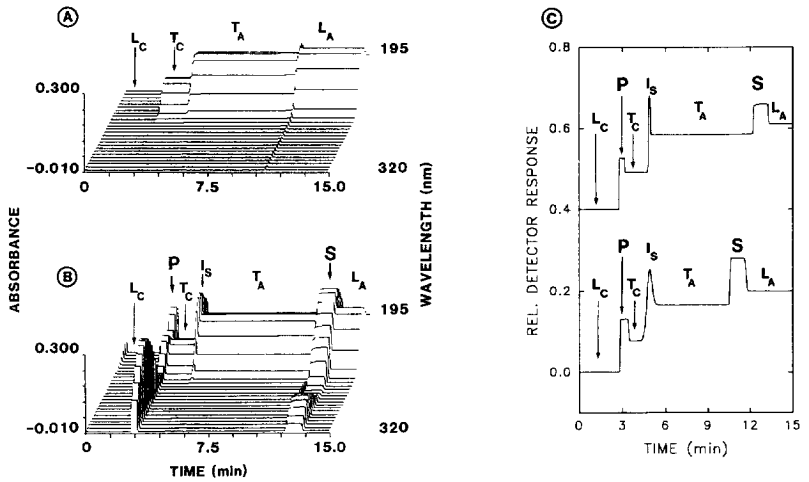

Fig. 5. Bidirectional multiwavelength cITP data of (A) blank and (B) procaine and salicylate at pH 6. The data presented in panel C depict computer-simulated (lower graph with converted time scale) and experimental pherograms (top graph, drawn with a y-axis offset of 0.4 AU) for detection at 220 nm. For explanation of the simulation data refer to text. Symbols are as for Fig. 2.

predicted to be about 10% lower compared to the case at alkaline pH (Fig. 6A, data for systems 2 and 3). Furthermore, some variation in the temporal behavior of this property is expected. The predicted current density as a function of time is presented in panel B of Fig. 6. Despite a lower steady state level being attained, the overall shape of the temporal behavior is similar to that predicted for system 3 of Table 2.

3.4. Bidirectional isotachophoresis at acidic pH

The third system investigated comprised a configuration with a pH distinctly below the pK_a of the capillary wall. β-Alanine and acetic acid were chosen as counter components in the anolyte and catholyte, respectively. The pH values of the two buffers were calculated to be 3.62 and 4.76, respectively (system 1 of Table 2). With simulations similar to those described above, electroosmosis was determined to be much smaller (about 1/5 compared to that at alkaline pH; Fig. 6A). A significant difference in the temporal behavior of the current density was also predicted. This property was found to decrease and level off at a rather low value (Fig. 6B). The computer-predicted data revealed an immediate loss of salicylate at the anodic end of the capillary and a gradual loss of procaine and the entire cationic zone pattern at the cathodic end. Thus, only procaine could be detected and a stationary steady state with the anionic terminating electrolyte (T_A) was produced (bottom graph in Fig. 7A). Electroosmosis appears to be insufficient for allowing the formation of the anionic zone structure within the capillary and for pumping it across the point of detection. Thus, this system was further investigated via application of cathodic, hydrodynamic co-flow. Computer-predicted flow data and corresponding current densities are presented in panels C and D, respectively, of Fig. 6. With a co-flow of 50 μm/s (net flow of about 65 μm/s), the distribution of current obtained is similar to that encountered at pH≥6 (Fig. 6B) and the zone distributions produced are also similar to those predicted for the previous systems studied (Fig. 8). Not surprisingly, a steady-state distribution with an anionic salicylate zone near the cathodic end of the column (chloride–salicylate boundary at about 90% of column length) and detection of both zone structures are predicted (top graphs in panels A and B of Fig. 7). The electropherograms depicted in panel B of Fig. 7 were obtained under the assumption that only salicylate and procaine are absorbing. The contributions (response factors) of the two compounds to the emulated detector signal were determined to be 55 and 70, respectively. Furthermore, with a co-flow of 25 μm/s (net flow of about 40

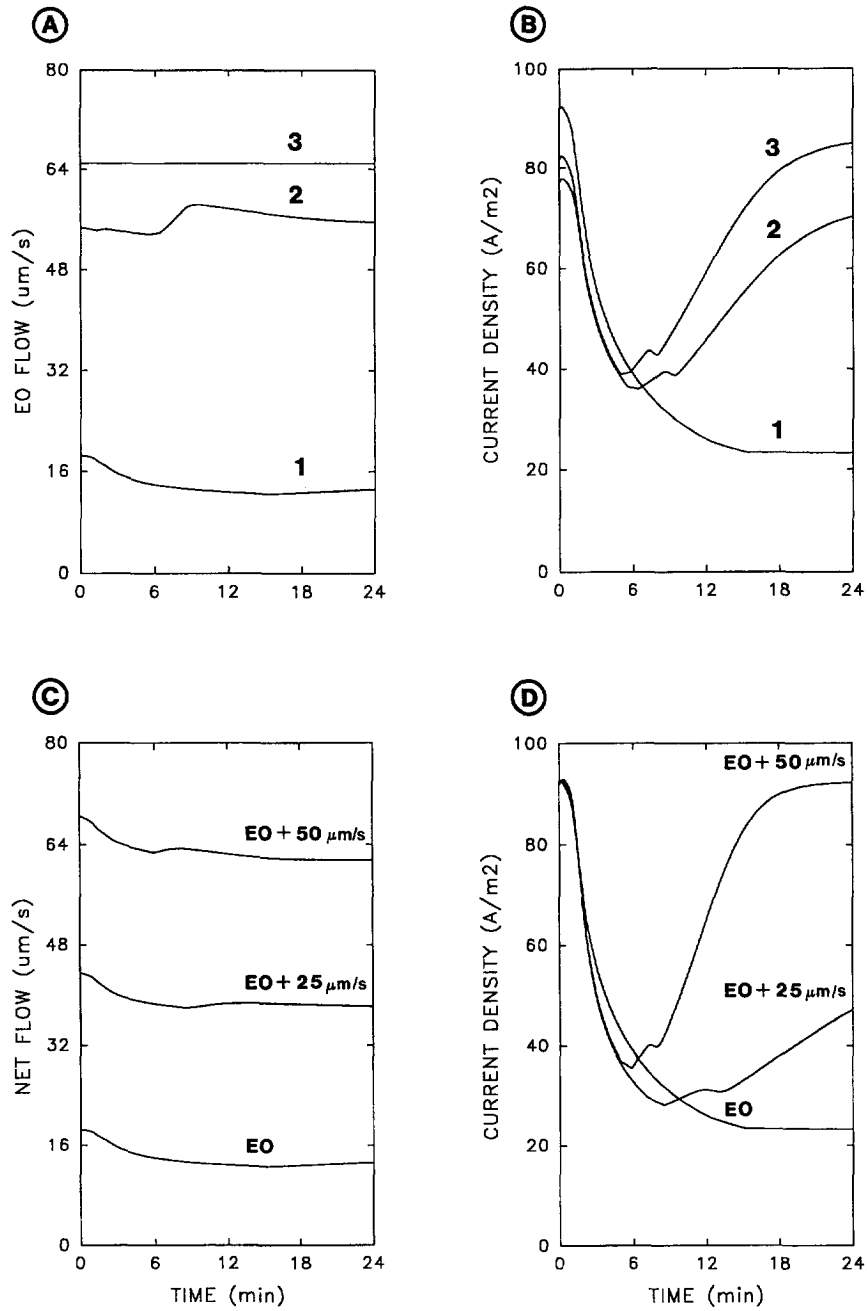

Fig. 6. Computer-predicted data for (A,C) net cathodic flow and (B,D) current density. The data presented in panel A represent the temporal behavior of the net electroosmotic flows for systems 1 to 3 of Table 2. Corresponding current densities as a function of time are depicted in panel B. Net cathodic flow data and current density data for system 1 with no co-flow (bottom graphs), a co-flow of 25 μm/s (center graphs) and 50 μm/s co-flow (top graphs) are presented in panels C and D, respectively.

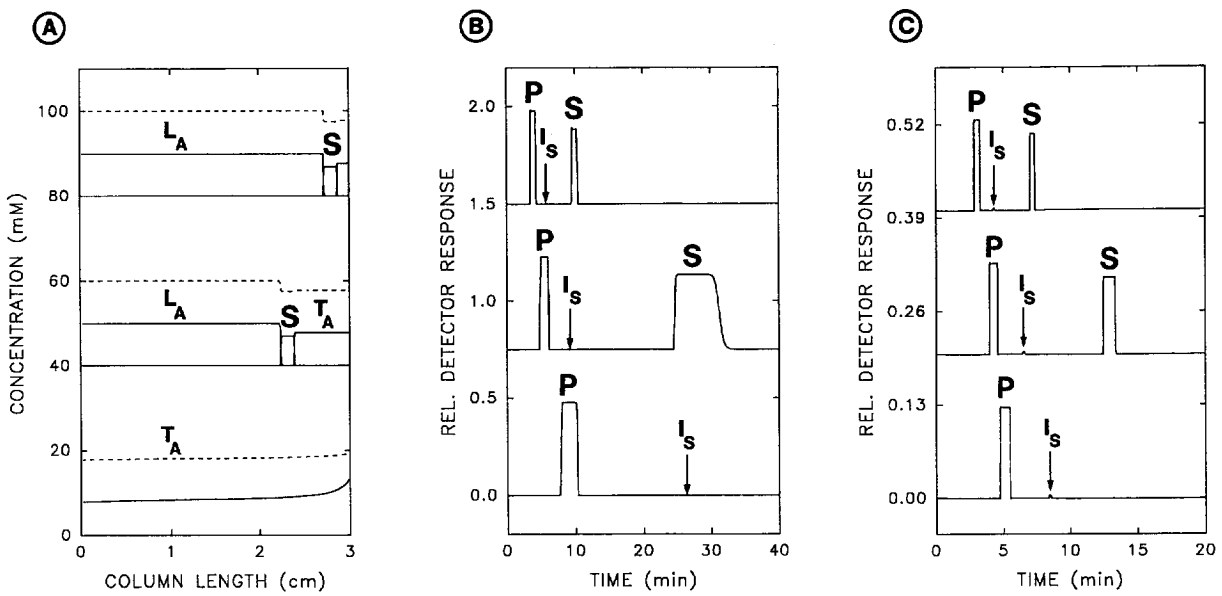

Fig. 7. Bidirectional cITP data at acidic pH (system 1 of Table 2). (A) Computer-predicted steady-state zone distributions after 40 min of current flow with 0, 25 and 50 μm/s imposed co-flow (from bottom to top, respectively; *y*-axis offset of 40 m*M*). The broken line represents β-alanine. (B) Corresponding computer-predicted electropherograms for 220 nm with a detector placed at 73% of column length. (C) Experimentally monitored electropherograms (220 nm) without application of co-flow (bottom graph), application of 20 mbar of positive pressure throughout the experiment (center graph, *y*-axis offset of 0.2 AU) and with 40 mbar of positive pressure (top graph; *y*-axis offset of 0.4 AU).

μm/s; Fig. 6C), an immobilization of the chloride–salicylate boundary at about 75% of the column length was obtained (center graph of Fig. 7A). Thus, with a detector placed at around 73% of column length, procaine and salicylate should be detectable (center graph of Fig. 7B).

Experimental data for this system are presented in panel C of Fig. 7. These data were generated by rinsing the capillary first with 0.1 *M* NaOH for 0.5 min prior to a 3-min wash with catholyte. In agreement with the computer simulation, data obtained without application of co-flow provided a peak for procaine, only. By applying 20 mbar of positive pressure throughout the experiment (co-flow of about 4.6 cm/min), both isotachophoretic zone structures could be monitored (center graph of Fig, 7C). The pattern observed is remarkably similar to that predicted with our model. The same applies for the data presented in the top graph of Fig. 7C, which were obtained with a co-flow of 9.2 cm/min (40 mbar positive pressure). These data underline the fact that there is qualitative agreement between the predicted and monitored zone patterns. This is also true for the applied flow. For the data presented in the center panels of Fig. 7B–C, the imposed co-flows per cm length of the column were 8.3 and 11.6 μm/s, respectively. Corresponding flows for the production of the top graphs were twice those values. It is important to note that the time axis scale of Fig. 7B is that resulting from simulation. Thus, differences in detection times are due to differences in applied voltage, capillary length, wall titration and capillary conditioning (see below). With data obtained at applied pressures of 10, 20 (Fig. 7C), 30, 40 (Fig. 7C) and 50 mbar, an average mobility $\mu = L_e/E\,t$, where L_e is the effective capillary length, t the detection time of the initial transition (marked as I_S in Fig. 7C) and E is the electric field applied, was calculated. Regression analysis of the five data pairs revealed a linear relationship between the average mobility and the applied pressure ($\mu = 0.115p + 1.95 \cdot 10^{-8}$ m^2/V s, where p is the pressure in mbar; $r = 0.999$). The obtained linearity suggests the absence of significant changes in the temporal

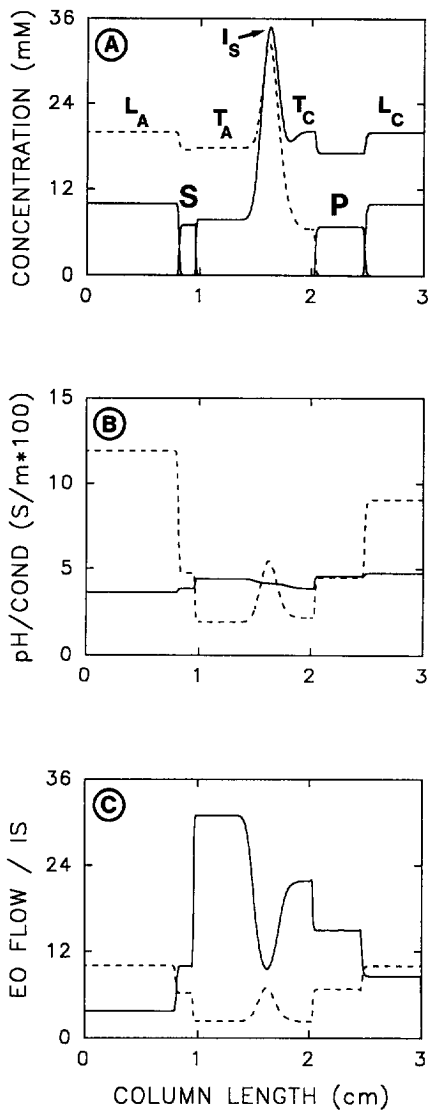

Fig. 8. Simulation data for system 1 of Table 2 with a co-flow of 50 μm/s and after 4 min of current application. (A) Concentration profiles with β-alanine being depicted as the broken line. (B) pH (solid line) and conductivity (broken line; units: S/m, values multiplied by 100) distributions. (C) Electroosmotic flow (solid line; units: μm/s) and ionic strength, IS (broken line; units: m*M*) data for each column segment.

behavior of electroosmosis. Furthermore, the intercept represents the average electroosmotic mobility of the system, i.e. $1.95 \cdot 10^{-8}$ m^2/V s. This value agrees well with the data presented in Fig. 1.

According to the simulation data with solute detection at 73% of column length, the conclusion can be reached that a net cathodic flow of ≥40 μm/s (flow relative to 1 cm capillary length of ≥13.3 μm/s) is required for monitoring of cationic and anionic zone structures. The limit is of course dependent on the point of detection. With detectors placed at an earlier position, the net flow can be somewhat lower (about ≥30 μm/s), whereas with instruments where the detector is placed closer to the end of the capillary, the net flow has to be significantly larger. For example, for detection at 90% of column length (as in many commercial instruments) a flow of >60 μm/s is required for detection of the anionic zone structure. An electroosmosis-based, cathodic displacement of this magnitude is predicted for alkaline systems only (Fig. 6A). For configurations around neutrality and at acidic pH, additional co-flow has to be applied.

3.5. Application to the monitoring of urinary salicylate and aspects of reproducibility

The bidirectional configurations 1 and 2 listed in Table 2 were evaluated for analysis of salicylate and its metabolites in human urine. Aspects of this topic have previously been investigated in our laboratory using anionic isotachophoresis [14] and micellar electrokinetic capillary chromatography [22] in untreated fused-silica capillaries. According to the metabolism of salicylate, significant amounts of urinary salicylate (S), salicyluric acid (SUA) and gentisic acid (GA) are expected [23]. In all systems studied, these substances were found to form anionic cITP zones and were detected between T_A and L_A, based upon their UV absorption and native fluorescence (Fig. 9). The data presented in Fig. 10 were obtained after direct injection of the urine of a patient with suspected salicylate intoxication into the bidirectional electrolyte system at pH 6. Zones within the anionic isotachophoretic stack could be assigned to the three compounds of interest, with identification being based upon spectral identity proofs (panel B) and simultaneous absorption and fluorescence detection (panel C). With the exception of the peaks marked as CA in the lower graph of Fig. 10A, the electrolyte system employed did not reveal any major cationic, UV-absorbing urinary compounds. When an acidic electrolyte system with a co-flow of 2.3 cm/min (induced by a positive

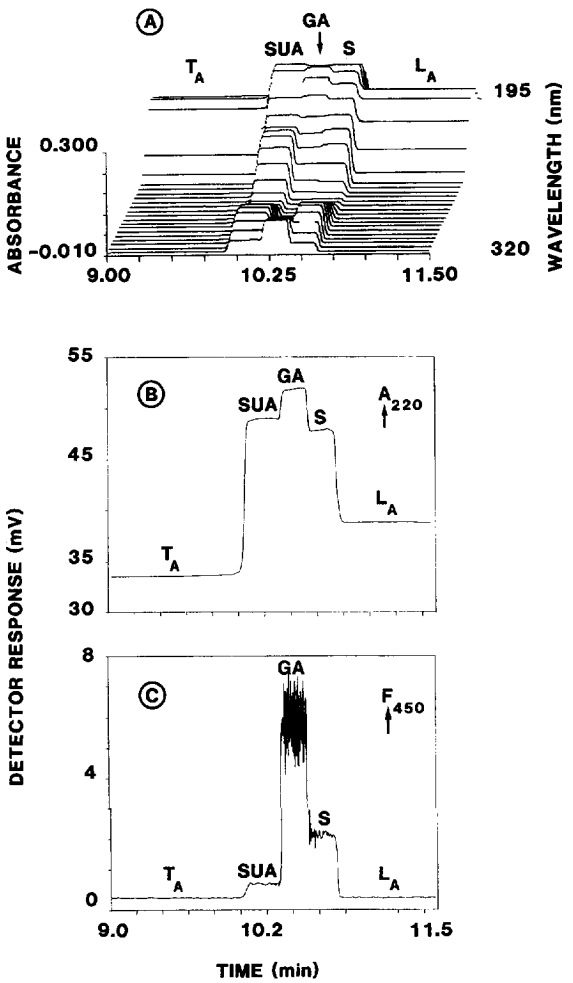

Fig. 9. Anionic cITP data at pH 6 (system 2 of Table 2) obtained with a model mixture comprising S, SUA and GA (2.5 m*M* each) and hydrodynamic sample injection at 80 mbar for 0.1 min. Electropherograms depicted include (A) multiwavelength absorption data, (B) absorption data at 220 nm and (C) fluorescence data at 450 nm.

pressure of 10 mbar) was used, the results were somewhat different. The multiwavelength data shown in panel A of Fig. 11 illustrate that, compared to the case at pH 6 (lower graph Fig. 10A), more UV-absorbing compounds migrate cationically. Moreover, the anionic stack is different too. This is best seen by comparing the data presented in Figs. 10C and 11B. Differences in the neutral part marked by I_S are also noticeable. Thus, the data presented reveal that pH-specific cutting of the urinary matrix into cationic, neutral and anionic compounds is achieved. Furthermore, the presence of a specific substance can be confirmed effectively by multiwavelength UV or combined absorption–fluorescence detection. It is interesting to add that under the given conditions, there were no fluorescing cationic and neutral compounds monitored.

Working with the configuration at acidic pH (system 1 of Table 2), day-to-day reproducibility was found to be severely hampered by significant changes in the magnitude of electroosmosis. Thus, the application of various rinsing procedures, including the use of a pH 9.2 solution containing 75 m*M* sodium dodecyl sulfate, which is similar to that suggested by Lloyd and Wätzig [24], and employment of a catholyte comprising 0.3% hydroxypropylmethylcellulose, was studied. With the latter approach, the net flow was reduced to the extent that a co-flow generated by ≥30 mbar was required for detection of the anionic zone structure at 73% of column length. Best results were obtained by rinsing the capillary first with 0.1 *M* NaOH for 0.5 min prior to the 3 min wash with the catholyte. For the analysis of a sample composed of 35 m*M* sodium salicylate and 100 m*M* procaine chloride in five consecutive runs (in the presence of co-flow generated by the application of 15 mbar of pressure), a steady increase in detection times of all boundaries and thus also of the zone lengths was observed from run to run. R.S.D. values for procaine and salicylate zone lengths were determined to be 4.2 and 11.7%, respectively. This instability does not appear to dramatically affect the cationic zone structure for which electromigrational and electroosmotic transport are in the same direction. The R.S.D. of the procaine zone length is comparable to that reported for cationic isotachophoresis at a pH value of around 5 [13]. However, reproducibility for the salicylate zone that migrates against electroosmosis is significantly lower. Depending on capillary conditioning, R.S.D. values >20% were also observed. For the other systems (Table 2), somewhat better data were obtained. Furthermore, working with urine as the sample, quantitation of anionic compounds could not be reliably achieved at any pH. It can thus be concluded that bidirectional isotachophoresis performed in untreated fused-silica capillaries with a single sensor placed towards the cathodic capillary

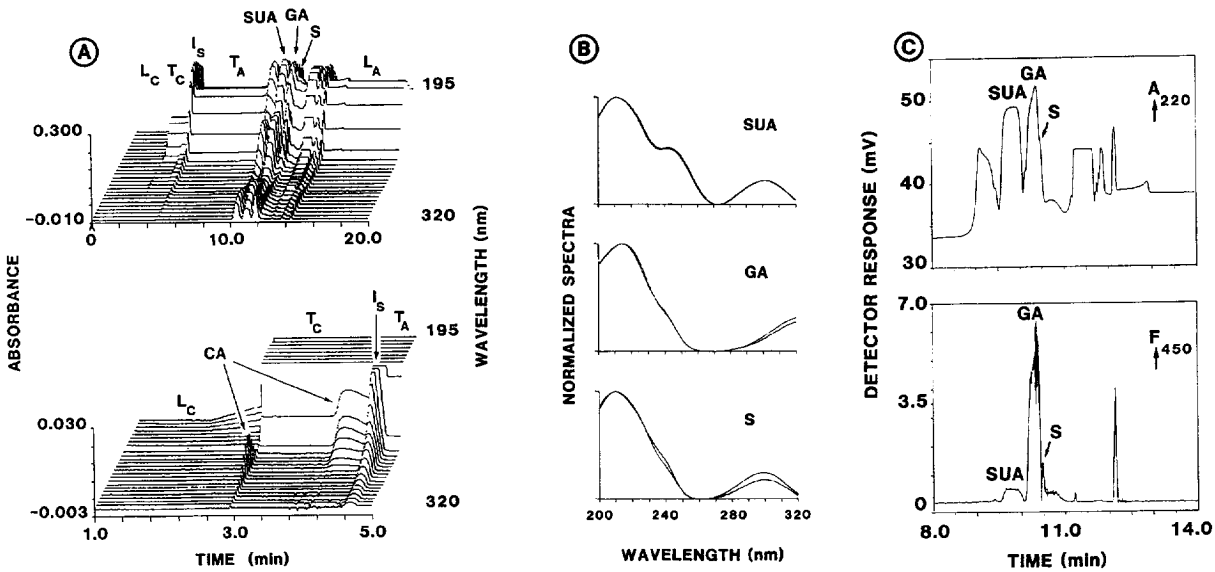

Fig. 10. Bidirectional cITP data obtained at pH 6 (system 2 of Table 2) and on direct injection of the urine of a patient with suspected salicylate intoxication as the sample. (A) Complete (upper graph) and cationic (lower graph) multiwavelength data. (B) Spectral identity proofs for S, GA and SUA showing normalized spectra extracted from the data of panel A and from the data of Fig. 9A. (C) Electropherograms resulting from the simultaneous gathering of absorption at 220 nm (upper graph) and fluorescence at 450 nm (lower graph). CA refers to cationic compounds.

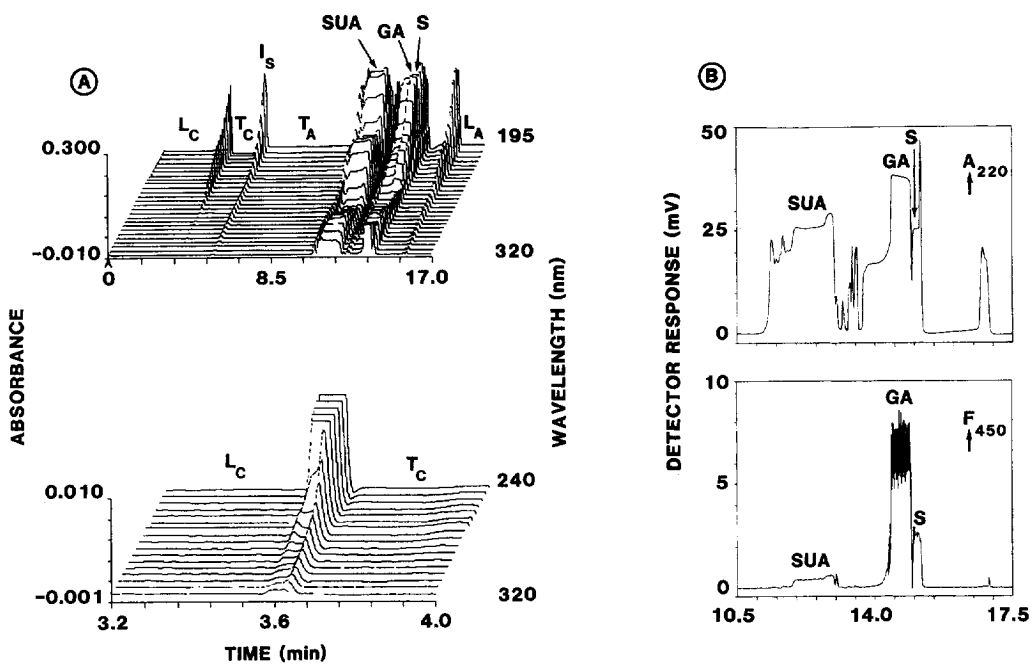

Fig. 11. Bidirectional cITP data obtained at acidic pH (system 1 of Table 2) with a co-flow generated by the application of 10 mbar of positive pressure and with the same sample as used for Fig. 10. (A) Complete bidirectional (upper graph) and cationic cITP (lower graph) multiwavelength data. (B) Simultaneously gathered 220 nm absorption data and 450 nm fluorescence data.

end is unsuitable for determination of accurate drug levels in body fluids. This approach, however, is perfectly suitable for screening and confirmation of drugs [14]. It is important to note that flow variations would not play a deleterious role for zone length measurements in instrumental configurations with linear array or fast scanning detectors along the column [25].

4. Conclusions

Computer-simulated bidirectional cITP data at acidic pH, around neutrality and under alkaline conditions are shown to agree well with those monitored experimentally using untreated open-tubular fused-silica capillaries of 75 μm I.D. With on-column solute detection at 73% of column length, cationic and anionic isotachophoretic zone structures can be detected, provided that there is a net cathodic flow per cm column length of about ≥10 μm/s. Based solely upon electroosmosis, this limit is attained at about pH≥6. At lower pH values, cathodic co-flow has to be applied for detection of anionic zone structures. With detectors placed at an earlier position, the net flow can be somewhat lower, whereas with instruments where the detector is placed closer to the cathodic capillary end, the net flow has to be significantly larger. For example, for detection at 90% of column length (as in many commercial instruments), a flow that is about 50% higher compared to that for 73% detection is required. An electroosmosis-based displacement of this magnitude is predicted for alkaline systems only. For all other configurations, additional co-flow has to be applied. The data shown in this paper have all been generated under constant voltage. As pointed out before [16], a run performed under constant current behaves different temporally but does provide the same final stationary zone distribution. Thus, the conclusions reached hold for configurations treated under constant current as well. Performing bidirectional cITP in fused-silica capillaries is shown to permit urinary confirmation of salicylate and two of its major metabolites via multiwavelength absorption detection or simultaneous absorption and fluorescence detection. Quantitation of urinary solutes, however, appears to be impossible with a single sensor placed towards the cathodic end of the capillary. Reproducibility at low pH is severely hampered due to a varying net flow caused by adsorption of solutes onto the capillary walls. Somewhat improved conditions are met at pH≥6.

Acknowledgments

This work was sponsored by the Swiss National Science Foundation.

References

[1] R.A. Mosher, D.A. Saville and W. Thormann, The Dynamics of Electrophoresis, VCH, Weinheim, 1992.
[2] L.G. Longsworth, in M. Bier (Editor), Electrophoresis, Vol. 1, Academic Press, New York, 1959, pp. 91–177.
[3] E. Schumacher and T. Studer, Helv. Chim. Acta, 47 (1964) 957 and references cited therein.
[4] W. Thormann, D. Arn, E. Schumacher, Electrophoresis 6 (1985) 10.
[5] T. Hirokawa, K. Watanabe, Y. Yokota, Y. Kiso, J. Chromatogr. 633 (1993) 251.
[6] T. Hirokawa, J. Chromatogr. A 686 (1994) 158.
[7] W. Thormann, J. Chromatogr. 516 (1990) 211.
[8] J.L. Beckers, F.M. Everaerts, M.T. Ackermans, J. Chromatogr. 537 (1991) 429.
[9] M.T. Ackermans, F.M. Everaerts, J.L. Beckers, J. Chromatogr. 545 (1991) 283.
[10] P. Gebauer, W. Thormann, J. Chromatogr. 545 (1991) 299.
[11] P. Gebauer, W. Thormann, J. Chromatogr. 558 (1991) 423.
[12] P. Gebauer, J. Caslavska, W. Thormann, J. Biochem. Biophys. Methods 23 (1991) 97.
[13] J. Caslavska, T. Kaufmann, P. Gebauer, W. Thormann, J. Chromatogr. 638 (1993) 205.
[14] J. Caslavska, S. Lienhard, W. Thormann, J. Chromatogr. 638 (1993) 335.
[15] H.R. Udseth, J.A. Loo, R.D. Smith, Anal. Chem. 61 (1989) 228.
[16] W. Thormann, J. Caslavska, R.A. Mosher, Electrophoresis 16 (1995) 2016.
[17] R.A. Mosher, C.-X. Zhang, J. Caslavska, W. Thormann, J. Chromatogr. A 716 (1995) 17.
[18] L. Steinmann, R.A. Mosher, W. Thormann, J. Chromatogr. A 756 (1996) 219.
[19] W. Thormann, S. Molteni, E. Stoffel, R.A. Mosher, J. Chmelík, Anal. Methods Instrumentation 1 (1993) 177.
[20] J. Pospíchal, P. Gebauer, P. Boček, Chem. Rev. 89 (1989) 419.

[21] M. Polášek, B. Gaš, T. Hirokawa, J. Vacík, J. Chromatogr. 596 (1992) 265.
[22] J. Caslavska, E. Gassmann, W. Thormann, J. Chromatogr. A 709 (1995) 147.
[23] J.-H. Liu and P.C. Smith, J. Chromatogr. B, 675 (1996) 61 and references cited therein.
[24] D.K. Lloyd, H. Wätzig, J. Chromatogr. B 663 (1995) 400.
[25] W. Thormann, J. Chromatogr. 334 (1985) 83.